Proceedings of the National Conference on Computational Modeling of Fluid Dynamics Problems (CMFDP-2019)
NIT Warangal, India – Jan 18-20, 2019
Paper No. XXX (The number assigned when the papaer is accepted)

Parametric Study of Aerostatic Bearing Performance Analysis With CFD Validation

Ayan Sarkar1[a], Santanu Sarkar2[b], Nripen Mondal3[c*]

[a,b,c]*Mechanical Engineering Department, Jalpaiguri Govt. Engineering College, Jalpaiguri, 735102, West Bengal, India*

*Corresponding author Email: nripen_mondal@rediffmail.com

Abstract

Aerostatic bearing is used in the recent times for the high precision applications like moment of inertia measurement system, coordinate measuring machine, dentist drill, high speed train etc. The advantages of the aerostatic bearing application is that it provide friction free movement between the static and rotating part and is also cleaner in the operation system compare to the conventional ball and oil bearing. The present study of this aerostatic bearing design has been considered with a centrally feeded air hole which is connected through an external compressor. The total supported load acts coaxially on the bearing rotor. The total mass flow goes radially through the gap between the bearing stator and rotor towards the atmosphere. The typical stator design has two circular pockets, one is at the centre of the stator and another just before the outlet. The objective of the present investigation is the parametric study of a stable bearing design which supports a heavy payload. The air bearing design modelling in the steady and dynamics is achieved by the numerical analysis in the Matlab -Simulink platform. The parametric study involved the different pressure supply with force capability, bearing stiffness, pressure profile at the gap etc. The numerical analysis is validated through the CFD analysis in Ansys Fluent which matches well with the analytical solution.

***Keywords*:** load capacity, stiffness, numerical analysis, CFD validation

1. Introduction

Aerostatic bearing are mainly used in the high precession applications moment of inertia measurement system, coordinate measuring machine, dentist drill, computer disk drive for the friction less and clean in operating condition[1-2].The very recently design of aerostatic bearing is for moment of inertia measurement system for heavy payload support during measuring air-bearing frictional free torsional oscillation.[3] The oil bearing would provide better stiffness but the operation system does not provide clean so new research dimension of air bearing [4]. The inherent orifice resistance flow of the bearing gap play the role of the bearing stability[5].The aerostatic bearing with multi-pocket orifice restrictor performance investigated by Yuntang et al[6].The various solution techniques for finding the pressure variation thin-film lubrication steady and transient investigated by Al-bender [7].The rectangular aerostatic bearing with centrally air hole feeding type of a computer slider has been analysed by Karkoub and Klkamel[8].They experimentally observed in an external pressurised air bearing the pneumatic hammer can be easily avoided by using small diameter orifices [9]. The CFD method aerostatic bearing performance investigated by Mohamed E and Eleshaky [10].They observed that bearing recesses pressure decrease which decreases the load bearing capacity as well as bearing stability performance. The counterbalance type aerostatic bearing analytical steady and transient model has been developed of the inherent resistance of the bearing passages analytical steady and model validated through CFD analysis [11].The recently simple perturbation flow of high thrust air-bearing model has been developed and validated through CFD moving mesh dynamic method[12].The objectives of the parametric study of the air-bearing analytical model and validated through the CFD analysis .

2. Air bearing geometry description and assumption

The figure 1 shows the sectional view of the air bearing design model. The total load (W) means payload plus the external weight which are acting coaxially of the bearing axis. The centrally feed air hole whose inlet is connected through external supply pressure p_c and the mass flow rate is $\dot{m}$ .The steeped feeder air hole design is with radius $r_1$for the length $L_1$and the rest of the length has radius is r_2.The air gap between the stator and payload support are two circular pockets. One is the inner circular pocket which radius is r_3 and air gap is (h_1+h_2) another pocket which located just before the outlet which radius is r_5 air gap is (h_1+h_2) rest of the radial direction air gap is h_1.The mass flow rate goes through the air hole to the radial direction gap between stator and payload to the atmosphere. During mathematical modelling the top gap different radial location r_2,r_3,r_4,r_5 andr_6 the pressure are p_{tin}, p_{tm}, p_{tm1} and p_{tout} respectively is considered. During the mathematical modellingthe following assumption are considered the flow is compressible, isothermal, flow between gap is laminar flow , the viscosity is constant and air obeys the ideal gas law.

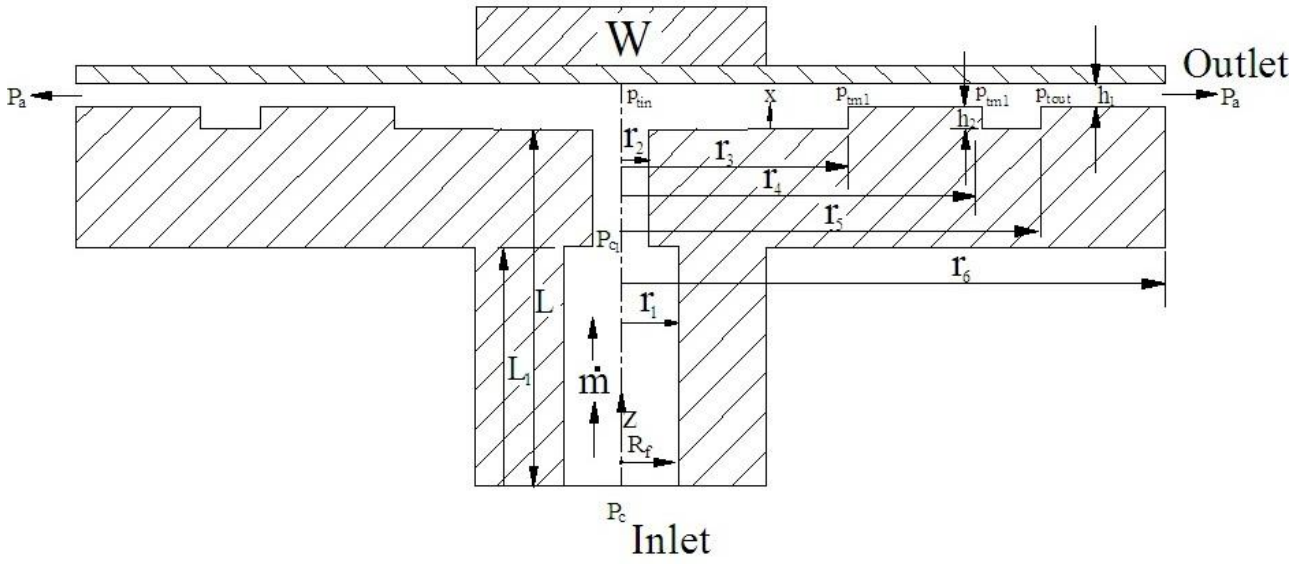

Fig 1: Sectional view of the aerostatic bearing

3. Air bearing mathematical modelling

The velocity profile through the bottom gap in isothermal condition written as

$$u_r = \frac{k_f \; x\left(h \; - x\right)}{r \; h} \tag{1}$$

Where *x* is the height from the stator top wall ,at wall *x*=0 then u_r=0, and *x=h/2* velocity will be maximum. The unknown parameter $k_f$is found out from continuity equation (2).

$$\dot{m} = \rho A u_r = \rho \int_0^h 2\pi r dx \, u_r \tag{2}$$

The unknown parameter $k_f = \frac{3\dot{m}}{\rho\pi h^2}$ (3)

The substituting the value k_f from equation (1) and find out the corrected velocity profile written as

$$u_r = \frac{3\dot{m}\, x(h-x)}{\pi\rho h^3 r} \tag{4}$$

After that apply ideal gas law and then rearranging the equation (4) can written as

$$u_r = \frac{3\,RT\,\dot{m}\,x(h-x)}{\pi\ p\ h^3 r} \tag{5}$$

Then Apply the Navier-Stokes equation with the following assumptions a) Steady State b) Axisymmetric problem and the velocity is only $u_r=f(x)$

Therefore N-S equations simplify to

$$\frac{1}{\mu}\frac{dp}{dr} = \frac{d^2 u_r}{dx^2} \tag{6}$$

$$\frac{1}{\mu}\frac{dp}{dr} = \frac{d^2}{dx^2}\left(\frac{3\,RT\,\dot{m}\,x(h-x)}{\pi p h^3 r}\right) \tag{7}$$

After rearranging the equation (7) can written as

$$dp = \frac{-6RT\,\dot{m}\,\mu}{\pi\ p\ h^3 r}\,dr \tag{8}$$

Then integrating equation (8) find out the expression for the radial pressure drops in the outer, outer pocket , middle and inner pocket gap segments. The expression for the different gap segments respectively can be written as.

The outer gap segment pressure drops expression

$$\int_{p_{tout}}^{p_a} d(p^2) = \frac{-12RT\,\dot{m}\,\mu}{\pi\ p\ h^3}\int_{r}^{r_6}\frac{dr}{r} \tag{9}$$

After performing the integration in the equation (9) and rearranging can be written as

$$p_{tout}^2 = p_a^2 + \frac{12\,RT\,\dot{m}\,\mu}{\pi\ h_1^3}\ln\left(\frac{r_6}{r}\right) \quad \text{for} \quad r_5 \le r \le r_6 \tag{10}$$

The outer pocket pressure drop expression can be written as

$$p_{tm}^2 = p_a^2 + \partial p_{tout}^2 + \frac{12\,RT\,\dot{m}\,\mu}{\pi\,(h_1+h_2)^3}\ln\left(\frac{r_5}{r}\right) \quad \text{for} \quad r_4 \le r \le r_5 \text{.....(11) and} \quad \partial p_{tout}^2 = \frac{12\,RT\,\dot{m}\,\mu}{\pi\ h_1^3}\ln\left(\frac{r_6}{r_5}\right)$$

The middle gap segment pressure drop can be written as

$$p_{tm1}^2 = p_a^2 + \partial p_{tout}^2 + \partial p_{tm}^2 + \frac{12\,RT\,\dot{m}\,\mu}{\pi\ h_1^3}\ln\left(\frac{r_4}{r}\right) \quad \text{for} \quad r_3 \le r \le r_4 \text{.....(12) and } \partial p_{tm}^2 = \frac{12\,RT\,\dot{m}\,\mu}{\pi\,(h_1+h_2)^3}\ln\left(\frac{r_5}{r_4}\right)$$

The inner pocket pressure drop can be written as

$$p_{tin}^2 = p_a^2 + \partial p_{tout}^2 + \partial p_{tm}^2 + \partial p_{tm1}^2 + \frac{12\,RT\,\dot{m}\,\mu}{\pi\,(h_1+h_2)^3}\ln\left(\frac{r_3}{r}\right) \quad \text{for} \quad r_2 \le r \le r3 \text{...(13) and } \partial p_{tm1}^2 = \frac{12\,RT\,\dot{m}\,\mu}{\pi\ h_1^3}\ln\left(\frac{r_4}{r_3}\right)$$

For the vertical branch of the hole, the flow is assume to be a component in the z direction of the hole axis and the hole radius is R_f. The velocity profile through this hole in isothermal condition satisfied the boundary condition and similarly like the previous process find out the pressure diffenent for the hole the equation can written as.

$$p_c^2 = p_{c1}^2 + \frac{8RT\mu\,\dot{m}\,L_1}{\pi r_1^4} \quad \text{for} \quad 0 \le L \le L_1 \tag{14}$$

And $p_{c1}^2 = p_{ti}^2 + \frac{8RT\mu \dot{m}(L - L_1)}{\pi r_2^4}$ for $0 \le L \le L - L_1$ (15)

The inlet supply pressure is P_c and the outlet is the ambient pressure P_a the total mass flow rate from, the inlet through the bearing passage can written as

$\dot{m} = \left[\frac{p_c^2 - p_a^2}{R_{gh}} \right]$ Where

$$R_{gh} = \left[\frac{12RT\dot{m}\mu}{\pi (h_1 + h_2)^3} \ln\left(\frac{r_3}{r_2}\right) + \frac{12RT\dot{m}\mu}{\pi h_1^3} \ln\left(\frac{r_4}{r_3}\right) + \frac{12RT\dot{m}\mu}{\pi (h_1 + h_2)^3} \ln\left(\frac{r_5}{r_4}\right) + \frac{12RT\dot{m}\mu}{\pi h_1^3} \ln\left(\frac{r_6}{r}\right) + \frac{8RT\mu\dot{m}L_1}{\pi r_1^4} + \frac{8RT\mu\dot{m}(L - L_1)}{\pi r_2^4} \right] \quad (16)$$

4. The static performance of the air bearing

The total net static force can be found by integrating the radial pressure. Since the steady state axial force balance condition can be written as,

$$F = \left[p_{tin} \times \pi\, r_2^2 + 2\pi \left\{ \int_{r_5}^{r_6} p_{tout}\, rdr + \int_{r_4}^{r_5} p_{tm}\, rdr + \int_{r_3}^{r_4} p_{tm1}\, rdr + \int_{r_2}^{r_3} p_{tin}\, rdr \right\} \right] \quad (17)$$

The static top gap dynamics of the combined load (W) written as

$$\ddot{h}_1 = g[F - W]/W \quad (18)$$

The air bearing axial stiffness can be define as the change of force capability with respect to change of air gap, the small change of air gap corresponding to the large variation of the force.

$$K = \frac{\partial F}{\partial h_1} \quad (19)$$

5. Result and Discussion

The numerically obtain all the result are presented here, the details of the air bearing configuration and bearing design parameters are shown in fig.1 and Table 1 respectively.

Table. 1. Air bearing design parameters

Symbol	Parameters description	Parameter value
h_1	Total air gap (m)	30×10^{-6}
h_2	Inner and outer pockets height(m)	0.0014
L	Feeder air hole total length (m)	0.035
L_1	Air hole length(m)	0.03
P_c	Supply pressure(Pa)	6×10^5,8×10^5,10×10^5
P_a	Ambient pressure(Pa)	1.1×10^5
R	Gas constant (KJ/Kg K)	287
r_1	Feeder hole radius (m)	0.005
r_2	Feeder hole radius(m)	0.0001
r_3	1st pocket outer radius(m)	0.015
r_4	2nd pocket inner radius(m)	0.025

r_5	2nd pocket outer radius(m)	0.26
r_6	Outer radius (m)	0.35
T	Ambient temperature (K)	293
μ	Viscosity of air (Ns/m^2)	0.00001820755

The total flow path resistance of the air-bearing is shows in fig.2 it has been observed that resistance decrease with increase of the air gap, from the equation (16) also it has been observed that the flow path resistance is independent of the inlet supply pressure.

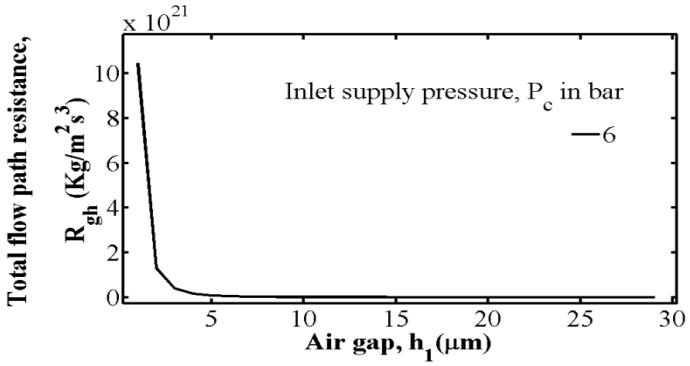

Fig.2. Total flow path resistance variation with air gap for fixed pressure P_c

The effect of the axial force capability in changing the inlet supply pressure for 30 micron air gap shows in fig.3. from this result it has been observed that force capability is increasing with increasing the inlet supply pressure.

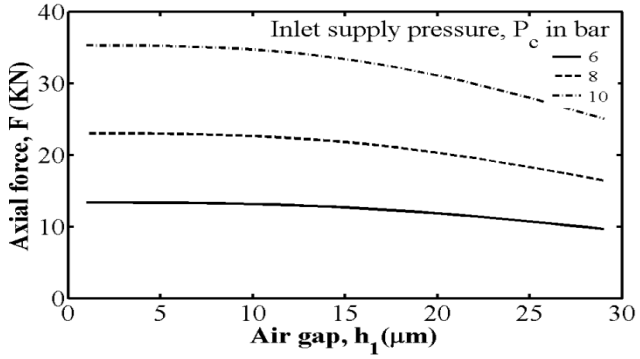

Fig.3. Axial force variation with air gap for different pressure P_c

The variation of the air bearing stiffness eqn.(19) with changing inlet supply pressure presented in fig.4. from this result it is observed that air-bearing stiffness increase with increase in the supply pressure and for different supply pressure stiffness monotonically decrease with increase in the air gap.

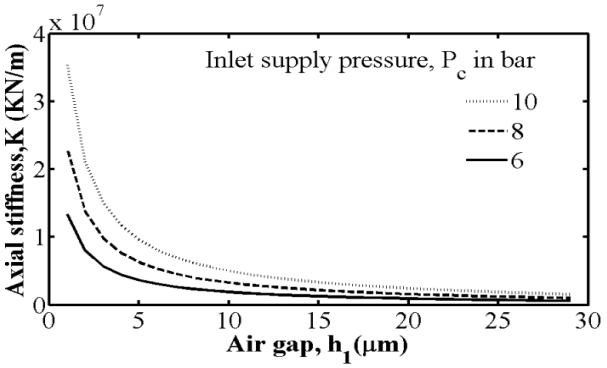

Fig.4. Axial stiffness variation with air gap for different pressure P_c

The mass flow rate variation for the different supply pressure is shown in fig.5. from this figure it has been shows that increase of the supply pressure mass flow rate increase with the increase in the air gap

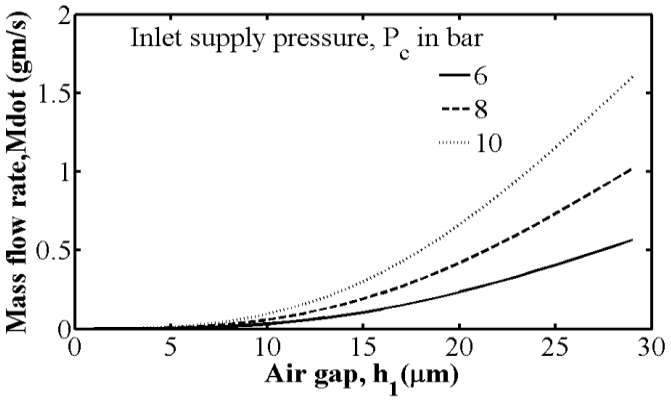

Fig.5. Total mass flow rate variation with air gap for different pressure P_c

The air gap pressure profile for the different supply pressure shows in fig.6 for 30 micron air gap, from this figure it's clear that radius r_2 to r_3 pressure is constant and radius r_3 to r_4 pressure decreases and radius r_4 to r_5 pressure remain constant again pressure decreasing to reach atmospheric pressure.

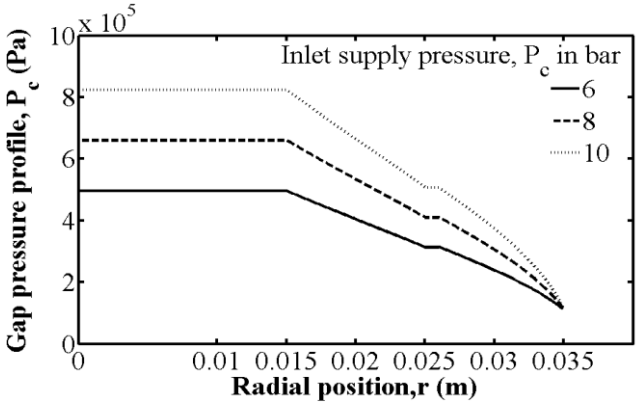

Fig.6.Gap pressure variation with radial location for different pressure P_c

The effect of the increasing outer radius r_6 from 0.03 m to 0.04 m axial force variation shows in fig.7 from figure it has been observed that force capability increasing with the increasing of outer radius.

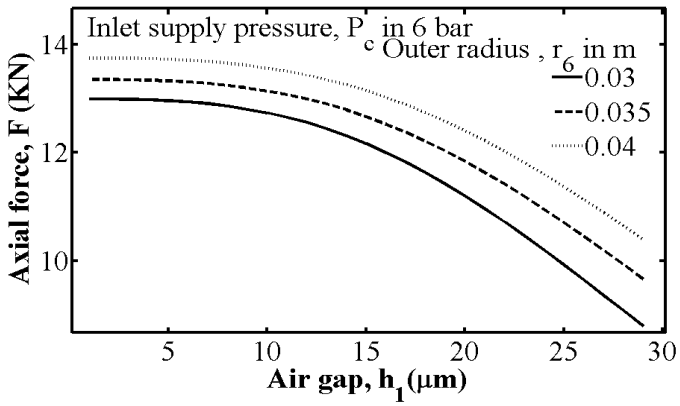

Fig.7. Axial force variation with air gap for changing outer radius in fixed pressure P_c

The effect of the outer pocket width changing for fixed supply pressure is shows in fig.8.

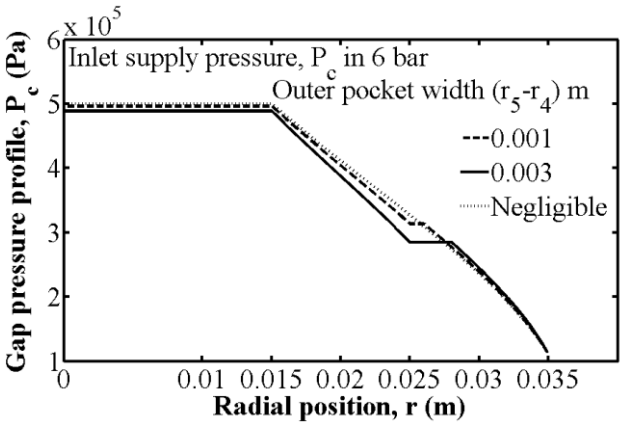

Fig.8. Gap pressure variation with radial location for changing outer pocket width

The similar effect has been made for the axial force capability is shows in fig.9 it has been seen that the force capability increase for negligible pocket width respect to others

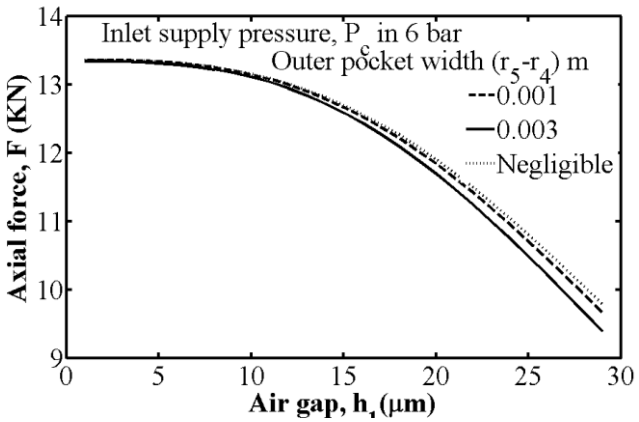

Fig.9. Axial force variation with air gap for changing outer pocket width

6. The validation of the analytical method with CFD result

The comparison between the analytical solutions obtained from the Matlab-Simulink platform and the CFD solutions obtained from the Ansys –Fluent 16. In the CFD solution Model it is considered Laminar flow, axisymmetric compressible flow isothermal and no-slip boundary condition the Navier Stokes equation flow air is consider for ideal gas. The second order discretization sheme has been considered. The validation of air bearing model the vertical air hole length L is 0.005 m and radius of inlet r_2 taken 0.0001m. and all other parameter remain same as table 1.The steady flow model is solved considering the inlet supply pressure 7 and 5 bar Matlab and CFD model the atmospheric pressure is the outlet boundary conditions. The total air gap between rotor and stator 30μm has been taken in Matlab as well as in CFD model. The validated CFD and analytical solution is quit matching and acceptable for the analytical model shown in fig.10.

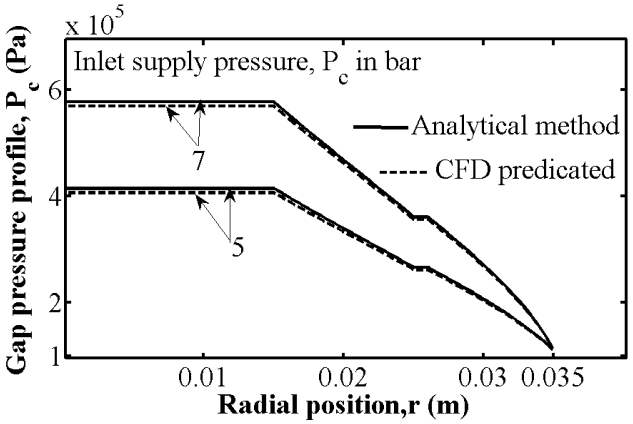

Fig.10. Validation of gap pressure analytical and CFD method

7. Conclusions

This paper is mainly focused on the steady analysis of the air bearing performance for varying the different input parameters likes inlet pressure, outer radius, outer pocket width etc. The flowing conclusion has been given below:

1) The air bearing force capability increasing with increasing the outer radius.
2) It has been also observed that when the outer pocket width reduces or eliminate the force capability slightly increases.
3) The air bearing axial stiffness increasing with increasing the inlet pressure.
4) The validation of the CFD and numerical model is accepted for the analytical solution method.

Acknowledgements

This research did not receive any specific grant from funding agencies in the public, commercial, or not-for-profit sectors.

References

1. H.Hashimoto, M.Ochiai, Y.Sunami, ASME J.Tribol.134(4), 032001(2012)
2. M.Kim, G.Jang, H.Kim, Tribol.Int.43(8),1479-90 (2010)
3. N.Mondal,S.Acharrya,R.Saha,D.Sanyal,K.majumder, Measument,78,309-321(2016)
4. B.X.Zuo,M.J.Wang,Q.Z.Yin and Y.S.Li, ASME J.Tribol.135(4),041701 (2013)
5. H.C.Chen,W.D.Yang, Y.Kang, Tribol.Int.44(4),368-379 (2011)
6. Li.Yuntang, and D. Han, Tribol.Int.56,66-71(2012)
7. F.Al-Bender precision Engg. 33,117-126(2009)
8. M.Karkoub and A.Elkamel, Tribol.Int.30,139-150 (1997)
9. M.H.Talukder and B.T.Stoweel, Tribol.Int.36(8),585-591(2003)
10. E. Mohamed and Eleshaky, Tribol.Int.42,1108-1117(2009)
11. N.Mondal,R.Saha,D.Sanyal, ASME J. Tribology,136,0317(2014)
12. N.Mondal,B.Saha R.Saha,D.Sanyal, ASME Journal of Dynamic Systems, Measurement, and Control,140,0410-8 (2018)